

Single-Nanocrystal Spectroscopy of White-Light-Emitting CdSe Nanocrystals

Albert D. Dukes, III,[†] Philip C. Samson,^{‡,||} Joseph D. Keene,[†] Lloyd M. Davis,^{‡,§} John P. Wikswo,^{‡,||,□,●,△} and Sandra J. Rosenthal^{†*,†,‡,||,⊥,||,△,▼}

[†]Department of Chemistry, Vanderbilt University, VU Station B Box 351822, Nashville, Tennessee 37235, United States

[‡]Vanderbilt Institute for Integrative Biosystems Research and Education, Vanderbilt University, Tennessee, United States

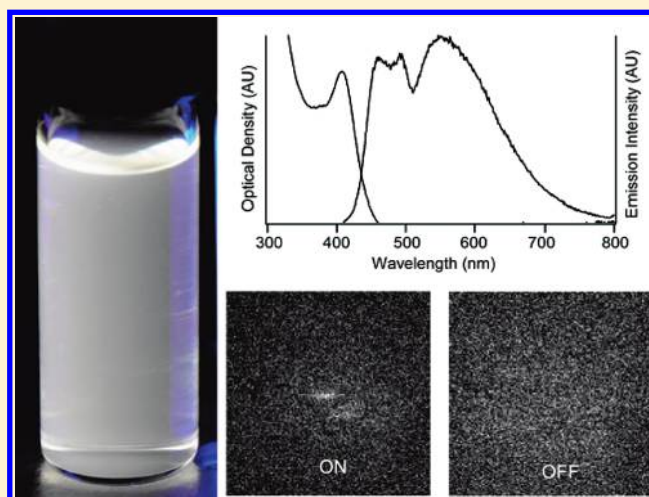
[§]Center for Laser Applications, University of Tennessee Space Institute, Tullahoma, Tennessee, United States

^{||}Department of Physics and Astronomy, [⊥]Department of Pharmacology, [□]Department of Chemical and Biomolecular Engineering,

[●]Department of Biomedical Engineering, [△]Department of Molecular Physiology and Biophysics, and [▼]The Vanderbilt Institute of Nanoscale Science and Engineering, Vanderbilt University, Nashville, Tennessee, United States

[⊥]Joint Faculty Oak Ridge National Laboratory, Oak Ridge National Laboratory, Oak Ridge, Tennessee, United States

ABSTRACT: We report the observation of broad-spectrum fluorescence from single CdSe nanocrystals. Individual semiconductor nanocrystals typically have a narrower emission spectrum than that of an ensemble. However, our experiments show that the ensemble white-light emission observed in ultrasmall CdSe nanocrystals is the result of many single CdSe nanocrystals, each emitting over the entire visible spectrum. These results indicate that each white-light-emitting CdSe nanocrystal contains all the trap states that give rise to the observed white-light emission.



INTRODUCTION

Ultrasmall nanocrystals, those with a diameter of less than 2 nm, have recently become an active research area as they have properties that differ markedly from larger nanocrystals.^{1–12} These properties include quantized growth,^{11,12} a size-independent emission spectrum,^{8,9} and white light-emission.^{2–7,10} Of these unique properties, white-light emission in CdSe nanocrystals has stimulated particular interest because of its potential for application in light-emitting diodes and solid state lighting applications requiring excellent color rendering.⁶

Ultrasmall CdSe nanocrystals have an almost pure white-light emission spectrum with chromaticity coordinates of (0.322, 0.365) on the 1931 CIE diagram.² As shown in Figure 1, white-light-emitting CdSe nanocrystals have a sharp band-edge absorption, indicating that the sample is monodisperse. The broad emission spectrum shown in Figure 1 is not typical of a monodisperse population of nanocrystals. While deep trap emission has been observed as a broad peak significantly red-shifted from the band edge, the three distinct peaks observed in the emission spectrum in Figure 1 are not observed in larger nanocrystals.

There are two possible explanations for the white-light emission observed in the ensemble spectrum shown in Figure 1. The first is that each CdSe nanocrystal has several different trap states on its surface required for white-light emission. The second scenario is that there are at least three energetically different trap states distributed among the entire population with each nanocrystal having distinct traps. This would result in the observation of each nanocrystal emitting only a narrow portion of the spectrum. To determine which explanation holds, we have designed and constructed a single-nanocrystal spectroscopy instrument.

Early work on the emission of white-light CdSe nanocrystals has determined that the emission spectrum is size-independent, or pinned.⁸ It was observed that the first emission feature ceased to blueshift once the band edge absorption reached 420 nm, though the band edge absorption continued to blueshift with

Special Issue: Graham R. Fleming Festschrift

Received: November 16, 2010

Revised: February 8, 2011

Published: February 22, 2011

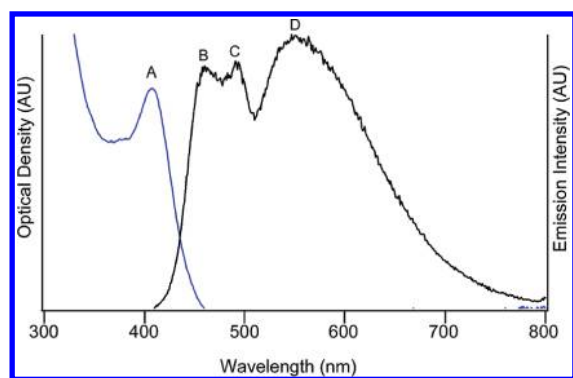


Figure 1. The ensemble absorption (blue curve) and fluorescence spectra (black curve) for the white-light-emitting CdSe nanocrystals are shown. The band-edge absorption peak is 408 nm (A). The narrow peak and sharp band-edge in the absorption spectrum indicate that the nanocrystal sample is monodisperse. The white-light fluorescence spans the majority of the visible spectrum with peaks at 450 nm (B), 490 nm (C), and 550 nm (D), resulting in a white-light emission spectrum.

decreasing nanocrystal diameter.^{8,9} This indicates that while the blue emission peak appears to be band-edge recombination, the peak is actually the result of trap-state recombination.⁸ Further work has demonstrated that the trap state involves the surface-passivating ligand, and that changing the ligand can change the wavelength of the blue emission peak.^{8,9}

Surface ligands are not the only way to modulate the white-light emission spectrum from CdSe nanocrystals.⁷ Quain et al. demonstrated that by allowing the reaction to proceed for longer periods of time, the emission color could be tuned from a warm white to a cool white.⁷ This was accomplished by slightly varying the time that the nanocrystals were allowed to grow. As the nanocrystals grew to larger sizes, the trap states responsible for the broad emission were eliminated. Additionally, nanocrystal growth resulted in a more pronounced blue emission peak. While white-light electroluminescence has been demonstrated,⁶ the work of Quain et al. indicates that it should be possible to tailor the emission of white-light-emitting diodes employing nanocrystals to consumer preference.

The emission properties of white-light-emitting CdSe nanocrystals were also investigated by Bowers et al., who utilized ultrafast fluorescence upconversion spectroscopy to determine the origin of the broad emission in this material.³ They conducted measurements at five wavelengths in the emission spectrum (459, 488, 535, 552, and 585 nm), while exciting the nanocrystals at 400 nm for each measurement. They observed that the radiative lifetime increased as the spectrum evolved from blue to red, similar to a fluorescent molecule. Bowers et al. concluded that much of the broad emission was the result of trap-state recombination. The shorter lifetimes were attributed to the extreme confinement of the white-light-emitting nanocrystals due to their diameter of 15 Å.³ In addition to the fluorescence upconversion studies, Bowers et al. imaged the white-light-emitting CdSe nanocrystals using aberration corrected scanning transmission electron microscopy. These images showed that the nanocrystals have defects in their crystalline structure, missing or extra atoms, which could create trap states.³

While the work performed by Bowers et al. established that the broad emission was the result of trap-state recombination, their technique was unable to interrogate individual nanocrystals and was reliant only on ensemble measurements. Left unanswered

was the question of whether each nanocrystal emits all three peaks, or if there is a distribution of distinct subgroups within the ensemble that are effectively monochromatic. If an individual nanocrystal emits only a portion of the ensemble spectrum, it is possible that this is the result of structural variations of the nanocrystals within the sample. However, if each nanocrystal emits the entire broad spectrum, it is likely that each nanocrystal has essentially the same structure.

In this study, we report the observation of broad spectrum, white-light emission from individual CdSe nanocrystals. The white-light-emitting CdSe nanocrystals are observed to blink, which is the classic signature of individual nanocrystal emission. Further, the light from the blinking nanocrystals is white and uniform. These results indicate that each white-light-emitting nanocrystal contains all the trap states needed for the white-light emission observed in the ensemble spectrum.

EXPERIMENTAL SECTION

CdSe Nanocrystal Synthesis and Purification. White-light-emitting CdSe nanocrystals were synthesized as previously reported.^{2,3} The following reagents were combined in a three-neck flask: 1 mmol of CdO (99.99%, Strem) with 6 g of trioctylphosphine oxide (TOPO, 90% technical grade, Aldrich), 4 g of hexadecylamine (HDA, 98%, Aldrich), and 2 mmol of dodecylphosphonic acid. The dodecylphosphonic acid was synthesized according to standard procedures.⁹ The flask was fitted with a bump trap, rubber septum, and temperature probe. The reaction mixture was stirred and purged with argon to 150 °C. The purge needle was removed and the reaction mixture was heated to 330 °C under an argon atmosphere until the mixture was clear and colorless.

A 0.2 M solution of Se-tributylphosphine (TBP) (Se, 200 mesh, Strem; TBP, technical grade, 97–99%, Aldrich) was prepared under an inert atmosphere. When the reaction mixture became clear and colorless, 5 mL of 0.2 M Se-TBP was injected into the reaction flask. The reaction was halted with an injection of 20 mL of butanol when the solution began to turn yellow. The flask was further cooled below 90 °C with compressed air. An aliquot was then withdrawn and diluted with toluene. The band-edge absorption was measured on a Cary Bio 50 UV-visible spectrometer, and the ensemble fluorescence spectrum was measured on an ISS PC1 photon-counting fluorometer.

The white-light-emitting nanocrystals were isolated by precipitation with methanol and collected by centrifugation. The supernatant was discarded and the resulting yellow pellet was dried and then dispersed in 5 mL of hexanol. Excess surfactant was collected from the hexanol solution by centrifugation. The remaining hexanol solution was decanted into a vial, and the nanocrystals were precipitated with methanol and collected by centrifugation. The supernatant was discarded and the remaining nanocrystals were dried and then dispersed in hexanes for single-nanocrystal spectroscopy measurements.

Sample Preparation for Single-Nanocrystal Spectroscopy. The concentration of the stock white-light nanocrystal solution was determined by UV-visible absorption spectroscopy. The extinction coefficient was calculated using the equations of Yu et al.¹³ Aliquots of the stock solution were then diluted with hexanes to a concentration ranging from 20 to 70 nM. The resulting solution was then sonicated for 30 min to break up any possible aggregates that formed during the precipitation steps of the cleanup procedure. A 200 μm thick fused silica coverslip

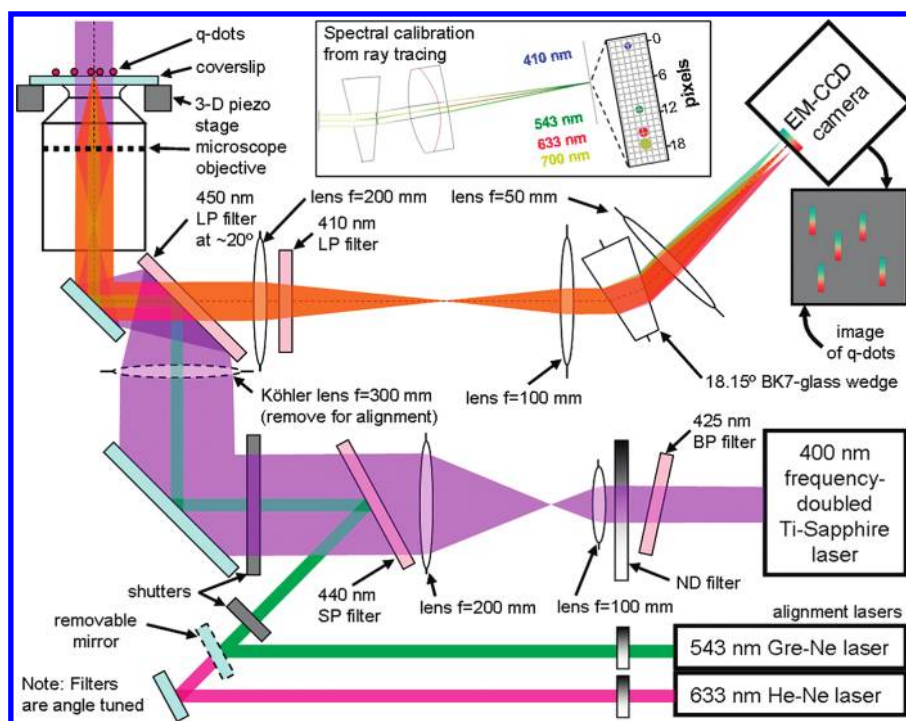


Figure 2. A schematic of the single-nanocrystal spectroscopy instrument. The 400 nm beam from a frequency-doubled Ti–Sapphire laser (shown in purple) is used for wide-field epi-illumination of a sample of CdSe nanocrystals. The emission from these is imaged onto a camera through a BK-7 glass wedge, which spectrally disperses the fluorescence in one dimension. The inset at top center shows ray tracing calculations from which the spectral calibration is determined. Light in the spectral band of 410–700 nm is dispersed in one dimension over 17 camera pixels. Beams from 543 or 633 nm lasers are used for initial alignment of the custom-built microscope and to check the spectral calibration.

(Structure Probe Inc., 01015-AB) was plasma cleaned with an air plasma to ensure a clean surface. A drop of the sonicated nanocrystal solution was added to the coverslip and the hexanes allowed to evaporate.

Single-Nanocrystal Spectroscopy Experiment. A schematic of the single-nanocrystal spectroscopy experiment is shown in Figure 2. The sample is excited with wide-field epi-illumination using the 400 nm beam from a frequency-doubled Ti-Sapphire laser. This is produced by using a 1 mm thick β -BBO crystal (Altos Photonics) for Type I angle-tuned frequency doubling of the 800 nm beam from a 76 MHz femtosecond Ti–Sapphire oscillator (Coherent Mira 900 Basic). The residual 800 nm light is removed by a 425 nm bandpass (BP) filter (Semrock, Bright-Line Fluorescence Filter 425/30), angle tuned so as to pass 400 nm. A neutral density (ND) filter wheel is used to attenuate the 400 nm laser power to 25 mW, measured immediately after the filter wheel. The 400 nm beam is expanded $\times 2$ and passed through an angle-tuned 440 nm short-pass (SP) filter (Semrock BrightLine Fluorescence Filter 440/SP). This filter blocks the residual 800 nm light not removed by the first filter and also functions as a dichroic mirror for bringing in either a 543 or a 633 nm beam from a GreNe or a HeNe laser. These beams are steered to be collinear to the 400 nm beam and are used for initial alignment of the custom-built microscope.

The 400 nm beam passes through a motorized shutter, which is closed to prevent photobleaching until just prior to data collection, then through a 300 mm focal length Köhler lens for wide-field illumination of the sample, and then is reflected from a 450 nm long-pass (LP) filter (Omega Optics, 3RD4500LP) to the microscope objective. The LP filter, which acts as a dichroic mirror, is angle tuned to $\sim 20^\circ$ resulting in 90% transmission at

450 nm. The objective (Olympus, 60 \times , water immersion, 1.2 NA, $\infty/0.13$ –0.21, FN 2.65, model: UPlanSApo), which has an effective focal length of 3 mm and pupil diameter of 7.2 mm, was rigidly mounted to produce an inverted microscope. Focusing is achieved by lowering the coverslip to the objective with a 3D piezo stage (Thor Laboratories, MAX301). Prior to the Köhler lens, the 400 nm beam has a diameter of ~ 1 cm. The Köhler lens focuses the beam within the microscope objective to a point about 6 mm below the coverglass so that the objective approximately recollimates the beam at the sample to produce an illumination disk of ~ 100 μm diameter.

Fluorescence collected by the objective passes through the dichroic, several lenses, a glass wedge (explained below), and a 410 nm LP filter (Omega Optics, 3RD410LP), which removes the residual 400 nm scattered excitation light that passes through the dichroic. The objective would produce a magnification of 60 \times if used in an Olympus microscope with tube-lens focal length of 180 mm, but here the fluorescence passes through lenses with focal lengths of 200, 100, and 50 mm, and hence the magnification for spatial imaging is 33.3 ($60 \times 200/180 \times 50/100$). Ultrasensitive fluorescence imaging is achieved by use of an electron multiplying charge coupled device (EM-CCD) camera with a back-thinned sensor for high quantum efficiency detection (Andor iXon^{EM+}, model: DU-897E-CSO-#BV). The pixel size of the camera is 16 μm , hence each pixel images a square sample area of 0.48 μm length and the 100 μm diameter illuminated sample region fills a region of ~ 200 camera pixels in diameter.

Initial experiments to image single nanocrystals were performed using an experimental setup without the glass wedge. On the basis of the observed signal strength in these experiments, it was decided to study the spectral features of single nanocrystals

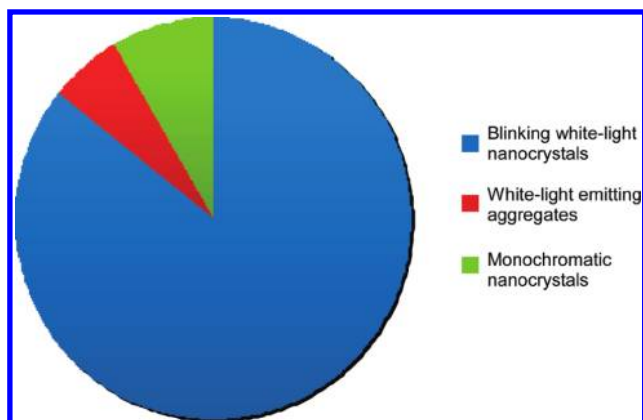


Figure 3. The pie chart shows the distribution of the different types of nanocrystals measured. The 216 blinking white-light-emitting nanocrystals are shown in blue. The 15 measured white-light aggregates are shown in red. The 21 measured monochromatic outliers are shown in green. The chart shows that 85% of the nanocrystals in the samples were blinking white-light-emitting nanocrystals.

by simultaneously imaging a field of many individuals using relatively low spectral dispersion/resolution, so as to achieve adequate signal-to-noise at each camera pixel. Hence a wedge made from relatively low dispersion BK7 glass, with an apex angle of 18.15° (Thorlabs PS814-A, AR Coating 350–700 nm) was chosen to disperse the emission. As seen in the inset at the top of Figure 2, ray tracing calculations using Zemax optical design software indicate that wedge disperses the spectral region from 410 to 700 nm over 17 camera pixels. The Airy disk diameter is 18 μm , approximately one camera pixel, consistent with experimental observations. The wedge is set at the symmetric condition of the angle of minimum deviation using the 543 nm green HeNe (GreNe) alignment laser. For alignment, the Köhler lens is removed so that the GreNe laser beam is focused to the top surface of the coverslip and the reflected portion is recollimated by the objective and passes back through the dichroic toward the wedge. After alignment of the lenses and wedge, the GreNe beam is attenuated and imaged onto the camera. The spectral dispersion is checked by replacing the 543 nm beam with the 633 nm alignment laser beam and noting the separation of the focal positions.

Spectral Imaging Conditions. With the Köhler lens providing wide-field illumination, the experiment geometry allows for the simultaneous collection of many nanocrystal spectra in a single measurement. For such measurements, the EM-CCD camera was thermo-electrically cooled to -50°C and the exposure time was set to 50 ms per frame. A low-laser irradiance ($\sim 200\text{ Wcm}^{-2}$) and high electron multiplier gain ($500\times$) were used to reduce photobleaching. Movies were collected with the camera operating in frame-transfer kinetic mode with 1000 or 10 000 frames in the series.

RESULTS AND DISCUSSION

The emission spectra of 252 nanocrystals from five separate batches were measured. As shown in Figure 3, 216 (85%) of the nanocrystals measured were individual white-light-emitting CdSe nanocrystals. The remaining nanocrystals were either white-light-emitting aggregates (15 measured aggregates) or monochromatic outliers (21 measured outliers). The only nanocrystals observed to not have the broad emission were the

monochromatic outliers. All of the broad emitting nanocrystals, aggregates and individual, span the entire spectrum. Nanocrystals that did not exhibit fluorescence intermittency were classified as aggregates. When a nanocrystal was observed to blink, the signature of single nanocrystal emission,^{14–16} the intensity at each pixel across the row for the blinking nanocrystal was recorded. The blinking nanocrystals observed here were dispersed over 15 pixels, or $\sim 250\text{ nm}$. When a nanocrystal was observed to blink in the movie, the intensity of each pixel was recorded starting at the red edge of the emission and spanning the visible spectrum toward the blue. Each collected spectrum was 18 pixels wide and a single pixel tall. The collected spectra are from a single 50 ms frame. When the spectra were analyzed, the onset of blue emission was assumed to be 450 nm (this wavelength is the wavelength of the first emission peak in the ensemble spectrum). Previous work has shown that this peak in the white-light-emission spectrum is pinned.⁸ Any emission below 450 nm is likely noise.

Several representative spectra are shown in Figure 4. While the spectra are noisy due to the small number of photons that can be collected from a single nanocrystal, it is clear that the individual nanocrystals have broad white-light emission. The observation of broad emission from individual white-light-emitting CdSe nanocrystals demonstrates that the trap states responsible for the emission are uniformly distributed to each nanocrystal. Figure 5 shows the summation of all 216 individual emission spectra. This combined emission spectrum resembles the measured ensemble spectrum shown in Figure 1. Further, this implies that each white-light-emitting CdSe nanocrystal has essentially the same structure. A trap state involving the surface passivating ligand has previously been shown to be responsible for the blue emission peak.^{8,9} The red emission peak resembles deep trap emission, which is the result of dangling bonds on surface Se atoms.¹⁷ The green (488 nm emitting) peak has been shown to be insensitive to ligand exchanges that involve ligands that bind to surface Cd atoms.⁸ This suggests that surface Se atoms are also involved in the process that leads to the green emission peak.^{3,8} Previous work by Bowers et al. determined that the decay of the population responsible for the blue peak resulted in the population of the state responsible for the red emission.³ Bowers et al. observed a multicomponent decay that when observed over the 50 ms integration of this work results in white light-emission from an individual CdSe nanocrystal. As shown in Figure 6, most of the nanocrystals are only on for one frame at a time. The intensity of the spectrum changes slightly from frame to frame, but the overall shape of the spectrum remains unchanged.

One of the limitations of the configuration of the instrument is its inability to establish the exact position of each nanocrystal whose spectrum is recorded. Monochromatic nanocrystals appear as single bright points on the camera. Since all the collected fluorescence passes through the wedge, and the nanocrystals are randomly distributed onto the coverslip, it would not be possible to determine the color of two different monochromatic emitters. To establish the color of two different monochromatic emitters, an image of scattered light of a single wavelength would need to be collected from each emitter. The displacement on the camera between the scattered light image and the fluorescent image could be calculated, and then the color could be determined. Because the CdSe nanocrystals used in this study are much smaller than the wavelength of visible light, this was not possible. It is very likely, however, that these outliers are blue emitters because CdSe nanocrystals of similar size have been reported to have blue emission.¹⁸

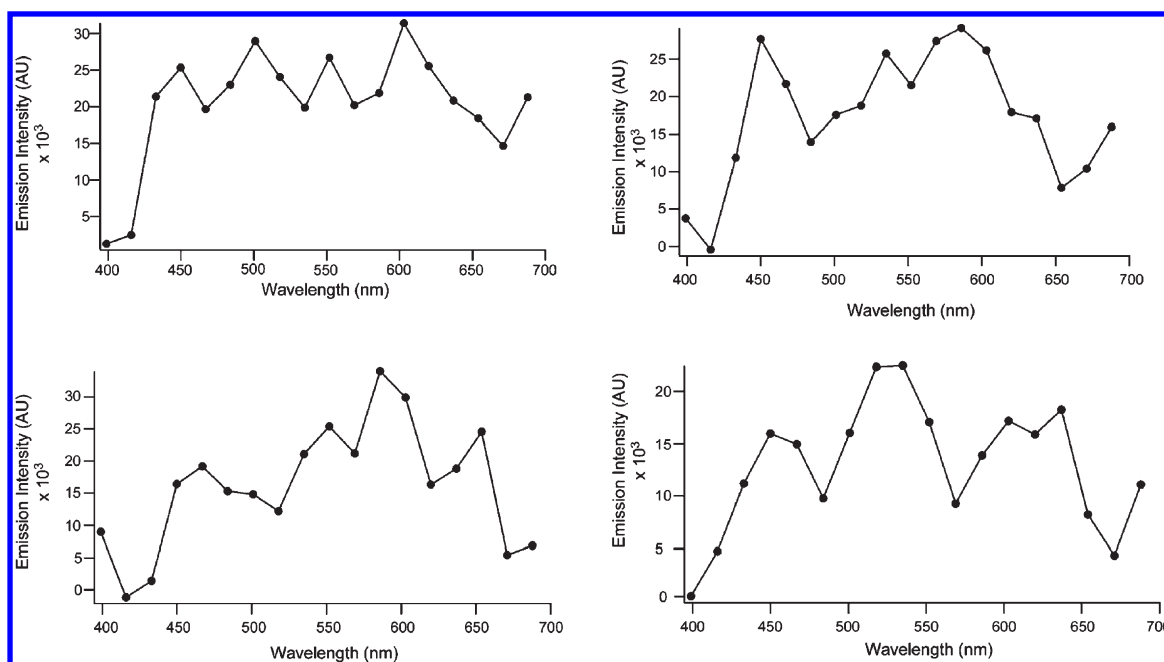


Figure 4. The broad emission spectrum of four different individual white-light-emitting CdSe nanocrystals is shown. The wavelength of each circle on the graph is the center wavelength for each pixel and has been connected by straight lines for clarity. These spectra show that the broad emission observed in the ensemble spectrum is the result of emission from individual nanocrystals that have several energetically distinct trap states that are responsible for the emission.

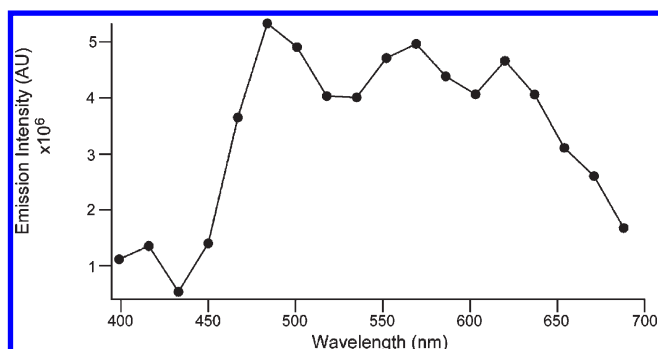


Figure 5. A composite emission spectrum of the 216 individual emission spectra measured is shown. The wavelength of each circle on the graph is the center wavelength for each pixel and has been connected by straight lines for clarity.

Previous studies have shown that the fluorescence spectrum of individual nanocrystals blueshift over time, which has been attributed to photo-oxidation of the nanocrystal.^{16,19} We were not able to observe such a blueshift in the white-light-emitting CdSe nanocrystals due to the limited spectral resolution of the experiment. Prior work showing that the emission spectrum of the ultrasmall CdSe nanocrystals is size-independent suggests that the emission spectrum should not blueshift with photo-oxidation.⁸

The integrated fluorescence signal as a function of time for a single white-light-emitting CdSe nanocrystals is shown in Figure 6. The white-light-emitting CdSe nanocrystals are in the OFF state much of the time, much longer than has been reported for larger, monochromatic nanocrystals.^{16,20} The extremely short ON times, shown in Figure 7, can be explained in the context of the Auger ionization model proposed by Nirmal et al.¹⁶ Fluorescence intermittency is the result of the nanocrystal emitting in a

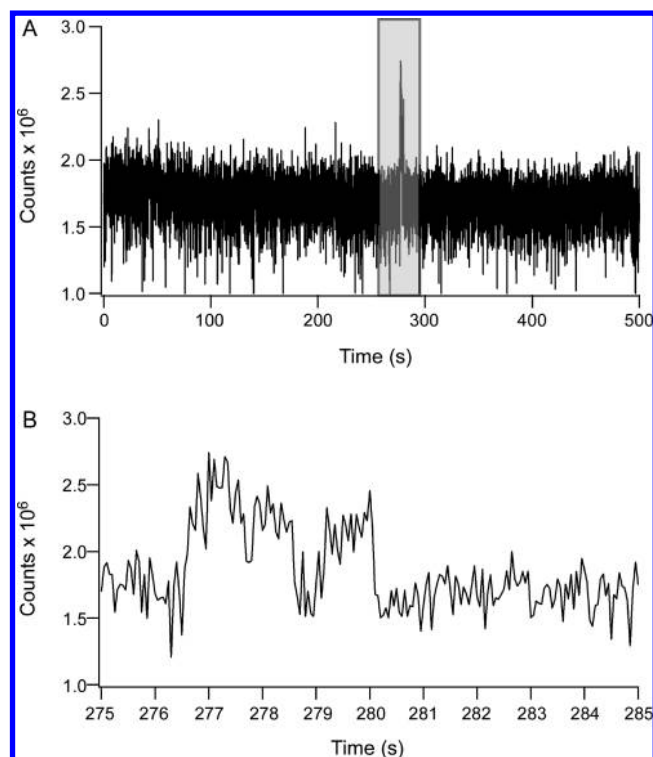


Figure 6. (A) The fluorescence intensity vs time for a single white-light-emitting CdSe nanocrystal. Data were collected for 500 s at 50 ms intervals. The ON state is highlighted in the gray box, which is expanded in (B).

charge neutral state (ON) and then transitioning to a charged state (OFF).¹⁶ Nirmal et al. have previously proposed a two-step ionization mechanism.¹⁶ In the first step, a carrier becomes

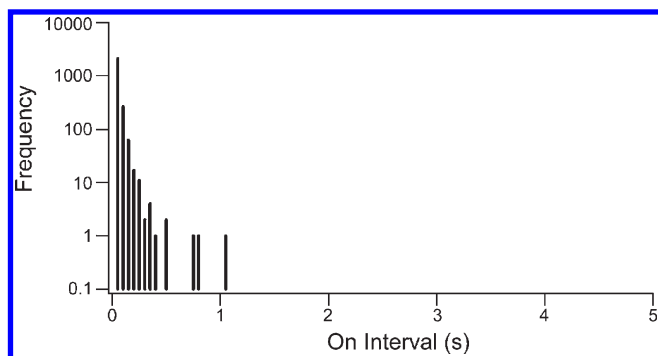


Figure 7. The histogram shows the frequency of the observed duration of the ON times for blinking white-light nanocrystals.

trapped on the nanocrystal surface. In the second step, the carrier is lost through photoionization within the trap state lifetime. Because of their extremely small diameter of 1.6 nm (as determined from the absorption spectrum),¹³ the white-light-emitting CdSe nanocrystals have a very high surface-to-volume ratio. Previous studies have estimated that as many as 70% of the atoms in a white-light-emitting nanocrystal are surface atoms, compared to 22% of the atoms located at the surface of 4 nm diameter nanocrystals.³ The resulting high concentration of surface trap states means that these states will quickly become populated. This will lead to a large population of carriers that can be photoionized and yield a charged (dark) nanocrystal in the OFF state.

CONCLUSION

We have shown that the emission of individual white-light-emitting CdSe nanocrystals is white. The white-light-emitting CdSe nanocrystals were observed to blink with all wavelengths emitting simultaneously. The nanocrystals are in a nonemitting state the majority of the time. This is the result of the extreme surface-to-volume ratio that leads to a high density of nonradiative surface trap states. This work shows that the trap states responsible for the white-light emission are present on each white-light-emitting CdSe nanocrystal.

AUTHOR INFORMATION

Corresponding Author

*E-Mail: sandra.j.rosenthal@vanderbilt.edu.

ACKNOWLEDGMENT

This work was supported in part through instrumentation funded by the National Science Foundation through Grants DMR-0619789 and EPS-1004083, the Vanderbilt Institute for Integrative Biosystems Research and Education. We thank Lumberline Laser, Inc. for donating the 543 nm Gre-Ne laser used during alignment. We also thank the de Jonge lab at Vanderbilt University for the use of their plasma cleaner.

REFERENCES

- (1) McBride, J. R.; Dukes, A. D., III; Schreuder, M. A.; Rosenthal, S. J. *Chem. Phys. Lett.* **2010**, *498*, 1.
- (2) Bowers, M. J.; McBride, J. R.; Rosenthal, S. J. *J. Am. Chem. Soc.* **2005**, *127*, 15378.

- (3) Bowers, M. J.; McBride, J. R.; Garrett, M. D.; Sammons, J. A.; Dukes, A. D.; Schreuder, M. A.; Watt, T. L.; Lupini, A. R.; Pennycook, S. J.; Rosenthal, S. J. *J. Am. Chem. Soc.* **2009**, *131*, 5730.
- (4) Gosnell, J. D.; Rosenthal, S. J.; Weiss, S. M. *IEEE Photonics Technol. Lett.* **2010**, *22*, 541.
- (5) Schreuder, M. A.; Gosnell, J. D.; Smith, N. J.; Warnement, M. R.; Weiss, S. M.; Rosenthal, S. J. *J. Mater. Chem.* **2008**, *18*, 970.
- (6) Schreuder, M. A.; Xiao, K.; Ivanov, I. N.; Weiss, S. M.; Rosenthal, S. J. *Nano Lett.* **2010**, *10*, 573.
- (7) Qian, L.; Bera, D.; Holloway, P. H. *Nanotechnology* **2008**, *19*, No. 285702.
- (8) Dukes, A. D., III; Schreuder, M. A.; Sammons, J. A.; McBride, J. R.; Smith, N. J.; Rosenthal, S. J. *J. Chem. Phys.* **2008**, *129*, 121102.
- (9) Schreuder, M. A.; McBride, J. R.; Dukes, A. D., III; Sammons, J. A.; Rosenthal, S. J. *J. Phys. Chem. C* **2009**, *113*, 8169.
- (10) Jose, R.; Zhelev, Z.; Bakalova, R.; Baba, Y.; Ishikawa, M. *Appl. Phys. Lett.* **2006**, *89*, No. 013115.
- (11) Kudera, S.; Zanella, M.; Giannini, C.; Rizzo, A.; Li, Y. Q.; Gigli, G.; Cingolani, R.; Ciccarella, G.; Spahl, W.; Parak, W. J.; Manna, L. *Adv. Mater.* **2007**, *19*, 548.
- (12) Zanella, M.; Abbasi, A. Z.; Schaper, A. K.; Parak, W. J. *J. Phys. Chem. C* **2010**, *114*, 6205.
- (13) Yu, W. W.; Qu, L. H.; Guo, W. Z.; Peng, X. G. *Chem. Mater.* **2003**, *15*, 2854.
- (14) Krauss, T. D.; Peterson, J. J. *J. Phys. Chem. Lett.* **2010**, *1*, 1377.
- (15) Kuno, M.; Fromm, D. P.; Hamann, H. F.; Gallagher, A.; Nesbitt, D. J. *J. Chem. Phys.* **2001**, *115*, 1028.
- (16) Nirmal, M.; Dabbousi, B. O.; Bawendi, M. G.; Macklin, J. J.; Trautman, J. K.; Harris, T. D.; Brus, L. E. *Nature* **1996**, *383*, 802.
- (17) Pokrant, S.; Whaley, K. B. *Eur. Phys. J. D* **1999**, *6*, 255.
- (18) Ouyang, J.; Zaman, M. B.; Yan, F. J.; Johnston, D.; Li, G.; Wu, X.; Leek, D.; Ratcliffe, C. I.; Ripmeester, J. A.; Yu, K. *J. Phys. Chem. C* **2008**, *112*, 13805.
- (19) Neuhauser, R. G.; Shimizu, K. T.; Woo, W. K.; Empedocles, S. A.; Bawendi, M. G. *Phys. Rev. Lett.* **2000**, *85*, 3301.
- (20) Shimizu, K. T.; Neuhauser, R. G.; Leatherdale, C. A.; Empedocles, S. A.; Woo, W. K.; Bawendi, M. G. *Phys. Rev. B* **2001**, *63*, No. 205316.